

Thermomechanical Performance of Shape Memory Alloy Spring by Homogeneous Distribution of Temperature

Husam Yahya Imran^{1*}, Dayang Laila Abang Abdul Majid¹, Mohd Faisal Abdul Hamid¹,
Ermira Junita Abdullah¹, Saleem Ethaib Mohammed², Sivasanghari Karunakaran¹

¹Department of Aerospace Engineering, Faculty of Engineering, Universiti Putra Malaysia,
43400 Serdang, Selangor Darul Ehsan, Malaysia

²College of Engineering, University of Thi-Qar, 64001 Al-Nassiriya, Iraq

ABSTRACT

In this paper, the thermomechanical characteristic behavior of a shape memory alloy (SMA) spring was studied. Under homogenous distribution of temperature by immersion in the hot and cold water, the thermal equilibrium of the SMA spring was obtained and its performance under different preloads applied was measured. The thermomechanical behaviors and properties of the SMA spring for one cycle were derived from the analysis of the displacement of contraction, pulling force produced and temperature versus response time through experimental tests. The experimental results showed that the performance of the SMA spring and the response time depend on the technique of the heating phase to activate it and the cooling phase to passivation it, as well as on the wire diameter and the preload applied. The maximum displacement contractions produced from 2.5 N and 1.5 N pulling forces for 0.51 mm and 0.38 mm wire diameter of the SMA spring were found as 49 mm and 35 mm respectively. The SMA spring was heated by increasing the temperature rate 0.3°C H/s of water and the temperature was decreased by adding cold water at a rate -6.1°C/s. The response time of the SMA springs that occurred at the temperature 74°C and 82°C were respectively 37 s and 50 s. The experimental results for both contraction-temperature and force-time responses at different preload, as well as collection of contraction-force-temperature responses to response time provide a good visualization as references for the design dimensioning and fabrication of the SMA spring as actuator, sensor and heat engine.

Keywords: Shape memory alloy spring, Reciprocal actuators, Performance sensors in heating water, Mechanical actuation of SMA spring

I. INTRODUCTION

Active materials are metallic materials with multiple engineering properties such as mechanical, thermal and also electrical. These properties are characterized by high strength and lightweight, which are used in various new and advanced applications [1]. One of the most common applications of active materials is that it can simultaneously act as sensor and actuator. The sensor converts mechanical signal (electrical or thermal) into voltage, whereas the actuator converts electrical energy into mechanical. Some examples of multifunctional active

materials include the piezoelectric, piezomagnetic and shape memory materials [2]. In brief, piezoelectric materials involve the coupling of mechanical and electrical, whereas the piezomagnetic materials include the coupling of mechanical and magnetic. Meanwhile, shape memory materials involve in the coupling of the thermal and mechanical fields.

In general, shape memory alloys (SMAs) are classes of intelligent materials which changes its crystal structure when exposed to a change in temperature. Recently, SMA is gaining wide interest in aerospace industry and medical fields due to the demand for actuation conditions with low-

grade temperatures such as for smart wings in aircraft and demonstration systems in jet engine [3-6]. These materials are characterized by their response to deformation in the cold martensitic phase and returning to their original form in the austenitic phase while maintaining the solid state in both phases without going through plasticity deformation of the metal [7]. The capability of these smart materials to return to their original shape when their temperature is increased is due to the shape memory effect (SME) which is producing force and contraction at the same time [8-10].

SMA is an alloy that consists of nickel and titanium, also known as Nitinol, possesses unique physical and metallurgical properties [11]. This material is characterized by its ability to deform plastically at room temperature and return to its previous shape before deformation when the material temperature is increased while maintaining its solid state in both phases [12]. Contraction and extension are the effects of the change in the crystal structure that occurs in the material when the temperature increases and decreases [13,14]. The SMA material gained popularity in various sectors of the industry such as nuclear, geothermal, automobiles, consumer devices, electronics and medical due to the exploitation of water temperature generated by the cooling systems [15].

Many researchers have investigated the capability of SMA material to modify and develop a new design of engine by using the new technology of manufactured material that has a high quality of performance such as Nitinol. It can be made to memorize some previously defined shape. The material can be deformed plastically, and when it is subjected to appropriate thermal conditions, it will return to the memorized shape [16]. The change in the shape of this material is the resultant of the material changing phase while still in a solid state. The alloys of NiTi and the copper-based alloys are most commonly used because these materials can recover substantial amounts of strain or generate significant force upon changing shape. Flexinol NiTi actuator is a commercial name of shape memory alloy that is becoming popular in the industry [17]. The only difference is that Flexinol has a better actuation property along the line of deformation compared to other SMA materials [18,19].

SMA material is a thermomechanical device (sensor or actuator) that generates different contractions and forces based on the shape, temperature and applied preload. This sensor or actuator cannot simultaneously produce maximum values for both contraction and force. The SMA spring generates maximum displacement of stroke with a minimum force, while the SMA wire produces maximum force with minimum displacement of stroke [20]. Additionally, the difference in the SMA performances is correlated with the heating technique, especially for the joule effect stream flow in SMA spring because of the inhomogeneous distribution temperature due to resistance of the material [21]. The maximum performance of the SMA spring is produced when it is activated by immersion of the spring in hot and cold water. The heating and cooling are represented by the thermal energy reserved in the SMA material. The activity of SMA is generated by increasing and decreasing temperature to operate the

actuator. However, the low operating frequency for the applications of SMA actuators is due to high relative heat capacity and density that leads to the difficulty in transferring the temperature rapidly [22,23].

The optimum cooling rates can be obtained from the SMA actuator when cooling in a fluid medium yet it still need a special design for preventing leakage into the environment [24]. The forced air for cooling the SMA actuator produces minor effects on the performance and some drawbacks like higher consumption of energy and noise production. In addition, active cooling cannot be practical for commercial applications because of its cost, weight, volume, as well as the control and mechanical complexity [25]. Some measures should be taken to prevent the SMA actuators from overheating, overstraining and overstressing to ensure safe performances over a large number of cycles (around 10^6 cycles). The maximum strain recommended should not exceed 3% to 4% strain and load 100 MPa [22]. The cycle period is defined as the total time of SMAs in heating and cooling. It is possible to control the heating time by changing the rate of heating. In opposite direction of the operation, the cooling time of SMAs should consider losing the temperature to the ambient [26]. There are several factors associated with cooling time such as the amount temperature, wire diameter of the SMA, the coefficient of thermal conductivity and the temperature of the operating ambient [27,28].

Most of SMA actuators are activated by transferring the temperature by means of conduction, convection, radiation or combination of those methods. Most common heating methods that can lead to the shape memory effect are by joule current, laser and water, whereas the cooling is carried out by forced air. However, there are several defects in these ways such as the limited passing of current may burn the SMA and requirement of higher consumption energy to increase performance due to the changing in the metallographic organization. Meanwhile, the heating by laser or hot air has a slow response and is uncontrollable due to center heating as a point on the surface of the SMA and lead to loss of thermal energy. These specific deficiencies of the SMA spring actuators require a new improved method such as by increasing and decreasing temperature through immersion of the SMA spring in water container to characterize its characteristic behavior and increase its response time in one cycle.

II. METHODOLOGY

The manufacturing of the SMA spring was carried out according to specifications of DYNALLOY, Inc, Makers of Dynamic Alloys Company, as tabulated in Table 1. The comparison and analysis of the characteristic properties of the two different SMA wire diameters in different preloads were conducted by measuring linear motion produced from the contraction and extension. The contraction and extension of wire is due to increasing and decreasing of the water temperature on which the wire is immersed in. The chosen SMA spring was the helical spring type due to its high-tension force ability of returning to the original shape by thermomechanical effects.

Table 1 Physical properties of the SMA spring [27]

| Symbol | Item | Value | |
|------------|-------------------------------|----------------------------------------------------|----------------------------------------|
| SMA | Shape memory alloy spring | Flexinol® (50% / 50%) ratio of nickel and titanium | |
| d | Wire diameter of SMA springs | 0.51 mm, 0.38 mm | |
| D | Outer diameter of SMA springs | 3.45 mm, 2.54 mm | |
| n | Number of active coils | 15 | |
| ρ | Density | 6.45 g/cm ³ | |
| c | Specific heat | 0.2 Cal/g * °C | |
| L | Latent heat of transformation | 5.78 Cal/g | |
| k | Thermal conductivity | 0.18 W/cm * °C | |
| α^A | Thermal Expansion Coefficient | Martensite | $6.6 \times 10^{-6}/^{\circ}\text{C}$ |
| α^M | | Austenite | $11.0 \times 10^{-6}/^{\circ}\text{C}$ |
| ν | Poisson Ratio | 0.33 | |

Significant specific temperatures of the SMA spring were denoted as A_s , A_f , M_s , and M_f (austenite start and finish transformation temperatures, and martensitic start and finish transformation temperatures). In the beginning, the SMA spring temperature was in low-temperature M_f . It was deformed plastically by the tension force of preload that occurred at the start transformation of increasing temperature and at the end transformation of twinned martensite at $T = 30^{\circ}\text{C}$ ($T > M_f$). When the temperature of water was increased gradually, the SMA spring contraction started and moved the preload by the tension force. This means the austenite transformation temperature A_s started at $T = 30^{\circ}\text{C}$ ($T < A_s$). The maximum displacement of the SMA spring contraction in the minimum period, followed by fluctuating contraction behavior representing the austenite A_f is finished at $T = 100^{\circ}\text{C}$ ($T > A_f$) as shown in Figure 1. At this point, the transformation of twinned martensite into austenite was gradually completed. The pulling tension force was also increased gradually due to the contraction of stroke in one

cycle of active and passive phase to the SMA spring by hot and cold water. The required response of the SMA spring actuation for the displacement contraction and force generated could be achieved through homogeneous temperature distribution via immersion in the water-changing temperature.

The thermomechanical test device of the SMA spring performance and actuation response were shown in Figure 2. The device can measure mechanical characteristics such as displacement of contraction and tension force produced from the SMA spring due to lifting of the preloads when the water temperature was increased and decreased. The prime components to be involved for the test include the IEC60825-1 2014 laser displacement sensor from Panasonic, which was used to identify the contraction (i.e., strain) in the SMA spring. A transducer kit load cell model with a capacity of 10 kg was used to determine the tension force exerted by the pulling force of the SMA spring to lift the weight. The K-type thermocouple was used to measure and monitor the water temperature to activate the SMA spring.

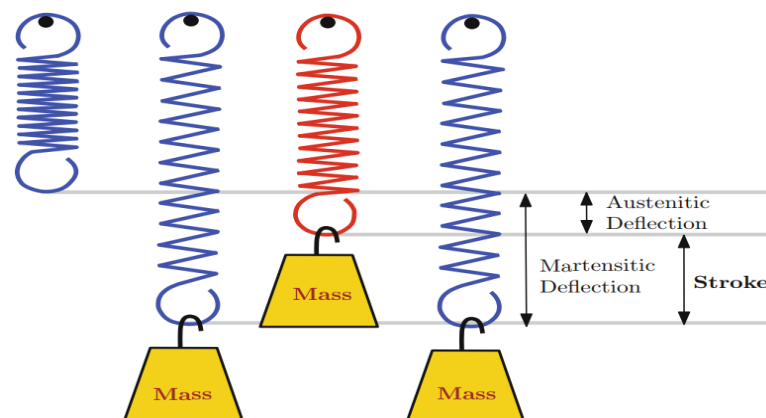


Figure 1 Austenitic and martensitic deflections of SMA spring [29]

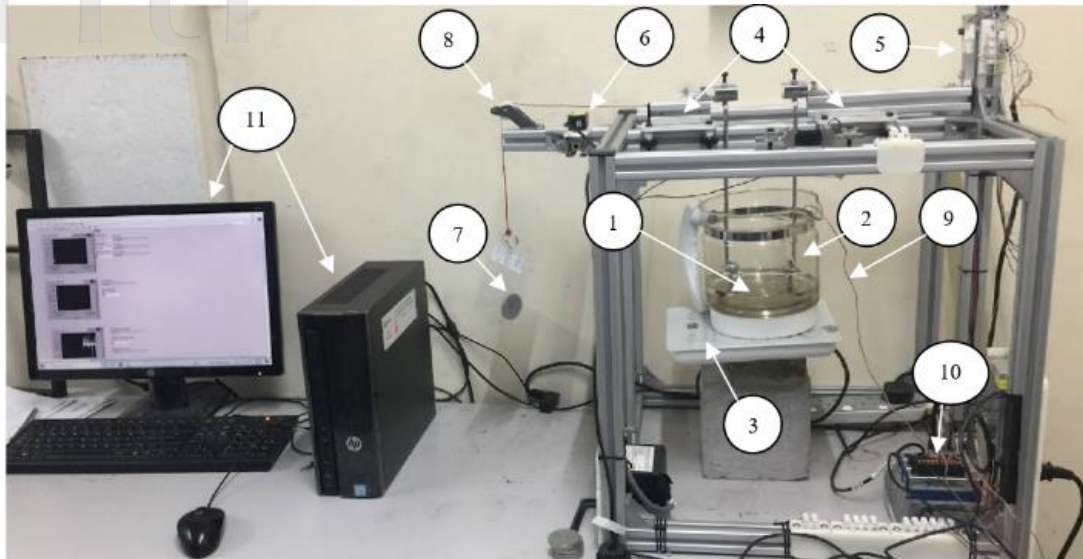


Figure 2 Assembly apparatus to measure the displacement and force resulting from activation of the SMA spring actuator

The experimental setup combines thermomechanical parts, which represent linear motion and force, and also electronic parts, which represent data collection for the behavior of the SMA spring when the temperature changes. Note that all essential components were denoted in Figure 2 and the following description was made with reference to this numbering. Thermodynamic experimental procedures were started by immersing the SMA spring actuator (1) in the water container (2) and the SMA spring contraction was driven by increasing the water temperature using an induction electric water heater (3). The two ends of the SMA spring were connected to two carts (4) that moved on a horizontal shaft through two vertical clamps. The first cart was connected to the load cell (5) to measure the tension force generated while the SMA spring contraction was identified by the laser sensor (6). The second cart was connected to the preloads (7) by a rope passing over the pulley (8). In addition, the K-Type of the thermocouple sensor (9) measured the temperature of the water. The National Instrument (NI) data acquisition system (10) was comprised of LABVIEW® software (11) to collect data in terms of force, displacement and temperature. Finally, the force data produced by the load cell due to displacement contraction of the SMA spring, data by the laser sensor and the source of activation temperature data of water by the k-type thermocouple were all collected by the LABVIEW software in the computer for later analysis.

This employed device mainly identified the relation between the displacement of the SMA spring contraction, tension force and temperature. The thermomechanical activation of the SMA spring was started by switching on the water heater from the normal temperature of 30°C before starting the test. A different preload was hanged for every test, which started from 1 N to 3.5 N by 0.5 N

increment. The water heater was switched off at 80 °C and all the experimental data were recorded.

III. RESULTS AND DISCUSSION

The SMA spring was immersed in water and was heated uniformly at a rate of 0.3°C H/s (Heating/s). It was observed that the initial change in length and slope was small due to the gradual increase in temperature. After that, a large change in length and slope occurred in the progress of attaining transformation temperature. The SMA spring was fully transformed into an austenitic phase and all the deflections that occurred was recovered. In the cooling cycle, the water temperature was decreased at a rate of -6.1°C C/s (Cooling/s) by adding cold water into the chamber. The SMA spring stretched to attain its previous length due to the preload tension and returned to the martensite phase in one complete cycle as depicted in Figure 3.

The experimental results of two SMA springs with diameter of 0.51 and 0.38 mm and different preloads applied in the same condition of increasing and decreasing water temperature highlighted the difference in the response time as represented in Figure 4. Furthermore, the relationship between the force and the increase in water temperature at different preloads as obtained from the experimental test is shown in Figure 5 for the SMA springs of diameter 0.51 mm and 0.38 mm. There were different A_s temperatures based on the preloads, which showed an increasing monotonous trend. In contrast, the response of A_f was not in a monotonous trend. It started with an increasing trend with increasing preload but after peaking at the optimum preload, the response started to decrease.

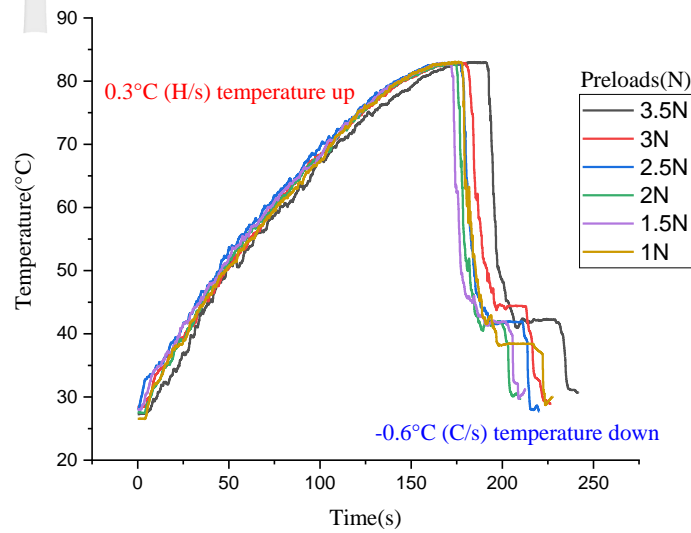
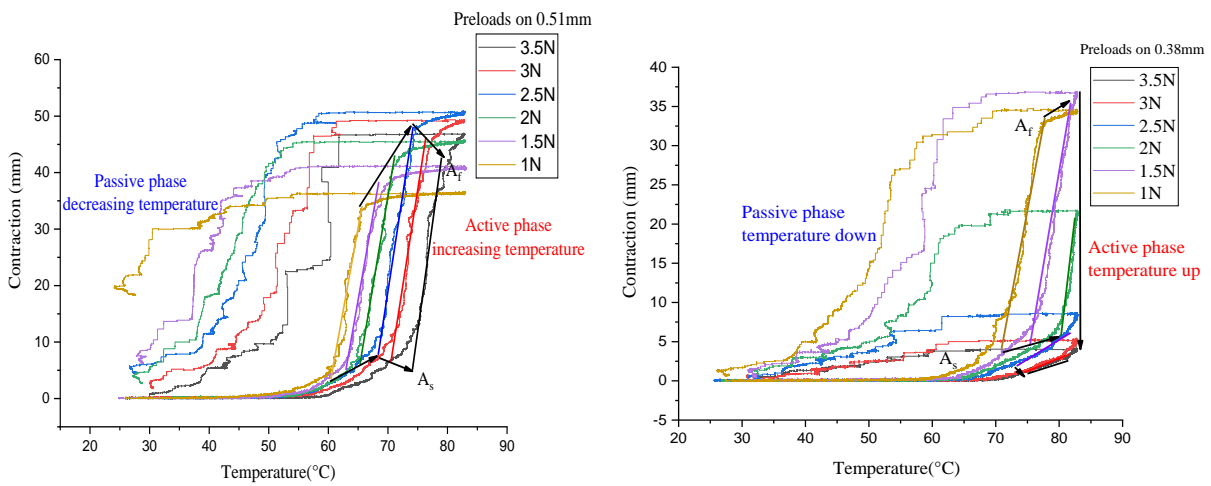


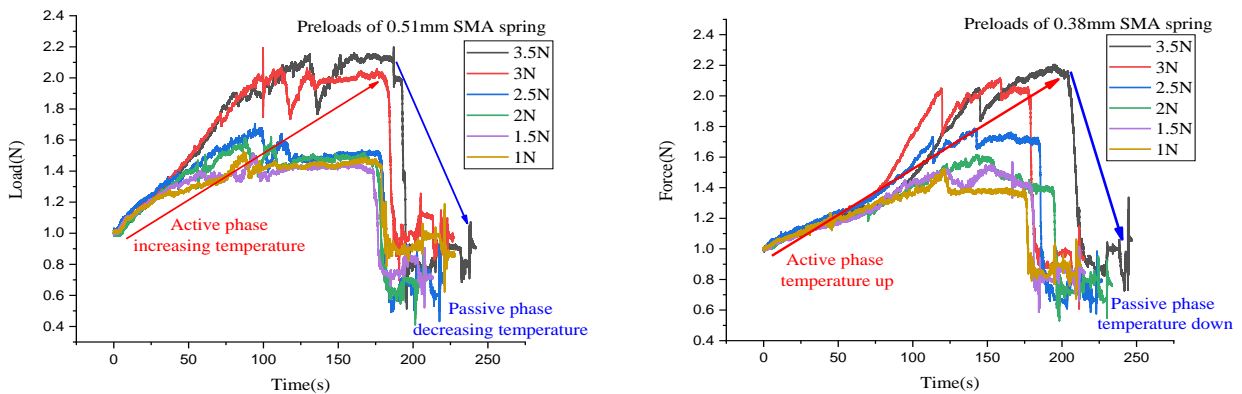
Figure 3 One cycle of increasing and decreasing water temperature of the SMA spring



(a) SMA spring with diameter of 0.51 mm

(b) SMA spring with diameter of 0.38 mm

Figure 4 Start and finish of contraction period in the austenite phase



(a) SMA spring with diameter of 0.51 mm

(b) SMA spring with diameter of 0.38 mm

Figure 5 Force generated from SMA springs in different preloads

In Table 2, the optimum contraction for an SMA spring with a diameter of 0.51 mm occurred at a preload of 2.5 N. For the SMA spring with a diameter of 0.38 mm, the optimum contraction occurred at a preload of 1.5 N as indicated in Table 3. When the SMA spring was activated using the hot water as smart thermomechanical actuators, it was necessary to identify the speed and output work in the applications. By estimating the displacement of SMA spring contraction versus temperature or time in active period, which was the power phase from A_s to A_f , it was easier to identify the speed of the activity and the work generated. This is presented in Table 4 based on the obtained results from the conducted experiment.

The SMA spring response time were correlated with optimum preload and temperature. For SMA spring with a diameter of 0.51 mm, the maximum contraction of 49 mm was achieved at preload 2.5 N with a response time of 37 seconds. Meanwhile, for SMA spring with a diameter of 0.38 mm, a maximum contraction of 35 mm was achieved at preload 1.5 N with a response time of 50 seconds. The

force produced from the SMA spring was dependent on the temperature of the thermal drive performance conducted in the test of the water heater setup. There were two important inflection points when the temperature was increased. When the water temperature was increased uniformly, it was noted the inflection curve of the force versus temperature changed in the behavior at A_s and A_f . When the temperature reached to A_s , the curve for the force dropped and then started to go up. The curve then started to drop again at A_f . This behavior can be observed in Figure 6, which indicates that the variation of contraction and force generated was nonlinear when the temperature of the SMA spring was increased in a constant rate. The uniform increase of the temperature produced continuous increase in the contraction and force between the A_s and A_f . In the meantime, in the sensitive temperature region between the A_s and A_f points, there were two inflection points in the SMA spring behavior. In each inflection point of contraction, the force degradation such as loss of stability and return increases regularly.

Table 2 The response properties of 0.51-mm SMA spring in different preloads

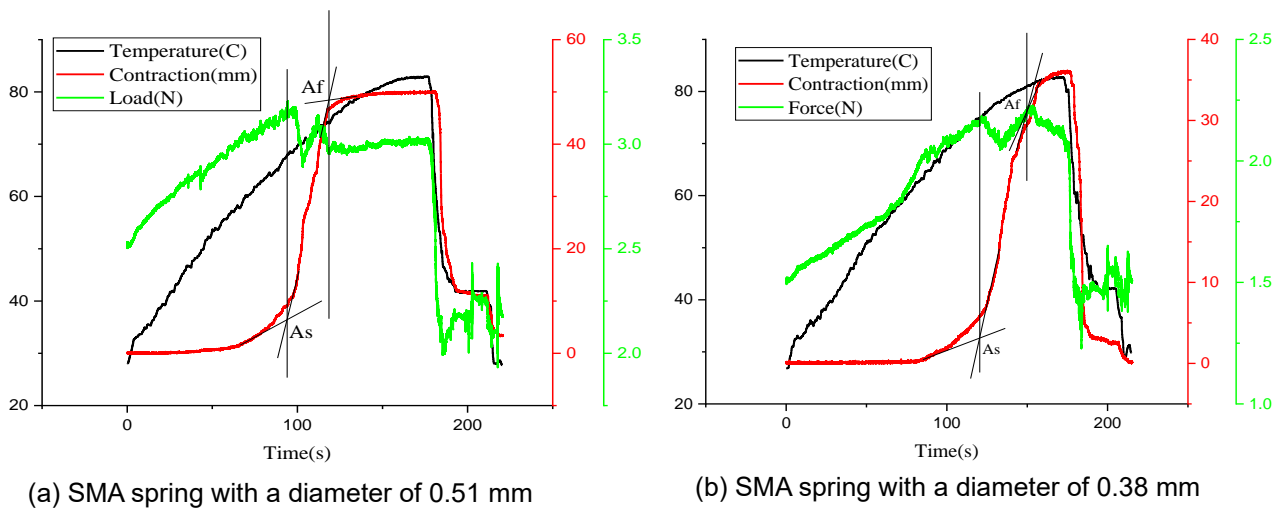
| Preload (N) | Temperature A_s (°C) | Time A_s (s) | Contraction A_s (mm) | Temperature A_f (°C) | Time A_f (s) | Contraction A_f (mm) | Contraction response (A_s-A_f) (mm) | Period response (A_s-A_f) (s) |
|-------------|------------------------|----------------|------------------------|------------------------|----------------|------------------------|-----------------------------------------|-----------------------------------|
| 1.0 | 61 | 77 | 4.7 | 65 | 96 | 34 | 29.3 | 19 |
| 1.5 | 63 | 78 | 5.5 | 68 | 100 | 38 | 32.5 | 23 |
| 2.0 | 65 | 87 | 5.8 | 71 | 115 | 43 | 37.2 | 28 |
| 2.5 | 68 | 88 | 6.8 | 74 | 125 | 49 | 42.2 | 37 |
| 3.0 | 72 | 96 | 7.3 | 78 | 136 | 47 | 39.7 | 40 |
| 3.5 | 74 | 112 | 7.6 | 80 | 161 | 45 | 37.4 | 49 |

Table 3 The response properties of 0.38-mm SMA spring in different preloads

| Preload (N) | Temperature A_s (°C) | Time A_s (s) | Contraction A_s (mm) | Temperature A_f (°C) | Time A_f (s) | Contraction A_f (mm) | Contraction response (A_s-A_f) (mm) | Period response (A_s-A_f) (s) |
|-------------|------------------------|----------------|------------------------|------------------------|----------------|------------------------|-----------------------------------------|-----------------------------------|
| 1.0 | 68 | 97 | 3.7 | 76 | 126 | 34 | 30.3 | 29 |
| 1.5 | 72 | 110 | 3.7 | 82 | 160 | 35 | 31.3 | 50 |
| 2.0 | 73 | 125 | 4 | 82 | 184 | 19 | 15 | 59 |
| 2.5 | 66 | 100 | 0.4 | 82 | 188 | 8 | 7.6 | 88 |
| 3.0 | 68 | 98 | 0.2 | 82 | 173 | 5 | 4.8 | 75 |
| 3.5 | 70 | 103 | 0.2 | 82 | 176 | 4 | 3.8 | 73 |

Table 4 Work produced and speed from homogeneous heating of the SMA spring

| Preload (N) | 0.51-mm SMA spring | | | 0.38-mm SMA spring | | |
|-------------|--------------------------------|------------|--------------|--------------------------------|------------|--------------|
| | Contraction (A_s-A_f) (mm) | Work (Nmm) | Speed (mm/s) | Contraction (A_s-A_f) (mm) | Work (Nmm) | Speed (mm/s) |
| 1.0 | 29.3 | 29.30 | 1.5 | 30.3 | 30.30 | 1.04 |
| 1.5 | 32.5 | 48.75 | 1.4 | 31.3 | 46.95 | 0.62 |
| 2.0 | 37.2 | 74.40 | 1.3 | 15.0 | 30.00 | 0.25 |
| 2.5 | 42.2 | 105.50 | 1.1 | 7.60 | 19.00 | 0.08 |
| 3.0 | 39.7 | 119.10 | 0.9 | 4.80 | 14.40 | 0.06 |
| 3.5 | 37.4 | 130.90 | 0.7 | 3.80 | 13.30 | 0.05 |

Figure 6 Response between A_s and A_f points at the optimum preloads for the SMA springs

IV. CONCLUSIONS

An experiment was carried out to identify the SMA spring activation characteristics, which was conducted in homogeneous distribution temperature by complete immersion in hot water. The shape memory effect in constant increase of temperature was monitored for two different wire diameters of SMA spring and different preloads. The thermomechanical characteristic of the SMA spring was represented by the displacement from the contraction and force produced to the response time in the power phase of activation. The results showed that the SMA spring produced a nonlinear behavior response for the contraction and force when temperature was increasing. For SMA spring with diameter of 0.51 mm, the maximum contraction of 49 mm was achieved at preload 2.5 N with response time of 37 seconds. Meanwhile, for SMA spring with a diameter of 0.38 mm, maximum contraction of 35 mm was achieved at preload 1.5 N with a response time of 50 seconds. Furthermore, the work generated and speed for moving this preload thermomechanical was 105 Nmm

and 1.14 mm/s for SMA spring with diameter of 0.51 mm. On the other hand, thermomechanical was 47 Nmm and 0.62 mm/s for SMA spring with diameter of 0.38 mm. All in all, this experimental characteristic response obtained from this study is useful as a reference in the design and fabrication of sensors, actuators and heat engine using this shape memory alloy.

ACKNOWLEDGMENTS

The authors would like to acknowledge the financial support from Geran Putra Siswazah, Universiti Putra Malaysia with project code GP-IPS/2021/9703000.

REFERENCES

- [1] Leal PB, Savi MA, "Shape memory alloy-based mechanism for aeronautical application: Theory, optimization and experiment," *Aerospace Science and Technology*, Vol. 76, 2018, pp. 155-163.

- [2] Schiller EH, Heat Engine Driven by Shape Memory Alloys: Prototyping and Design. PhD Thesis, Virginia Tech, 2002.
- [3] Abdullah EJ, Majid DL, Romli FI, Gaikwad PS, Yuan LG, Harun NF, "Active control of strain in a composite plate using shape memory alloy actuators," *International Journal of Mechanics and Materials in Design*, Vol. 11, 2015, pp. 25-39.
- [4] Oehler SD, Hartl DJ, Lopez R, Malak RJ, Lagoudas DC, "Design optimization and uncertainty analysis of SMA morphing structures," *Smart Materials and Structures*, Vol. 21, No. 9, 2012, 094016.
- [5] Sofla AYN, Meguid SA, Tan KT, Yeo WK, "Shape morphing of aircraft wing: Status and challenges," *Materials & Design*, Vol. 31, No. 3, 2010, pp. 1284-1292.
- [6] Chung KM, Huang YX, Chen WH, Liao YT, Huang JM, "Aerodynamic characteristics of a standard dynamics model in a spinning motion," *Journal of Aeronautics, Astronautics and Aviation*, Vol. 54, No. 2, 2022, pp. 215-226.
- [7] Gédouin PA, Pino L, Chirani SA, Calloch S, Delaleau E, Bourgeot JM, "R-phase shape memory alloy helical spring based actuators: Modeling and experiments," *Sensors and Actuators A: Physical*, Vol. 289, 2019, pp. 65-76.
- [8] Rao A, Srinivasa AR, Reddy JN, Design of Shape Memory Alloy (SMA) Actuators. New York, Springer International Publishing, 2015.
- [9] Awang Jumat N, Ogunwa TT, Abdullah EJ, Chahl J, Romli FI, Abdul Majid DL, "Flapping actuation using temperature feedback control of coated shape memory alloy actuators," *Microsystem Technologies*, Vol. 27, 2021, pp. 3299-3311.
- [10] Marimuthu N, Abdullah EJ, Majid DL, Romli FI, "Conceptual design of flapping wing using shape memory alloy actuator for micro unmanned aerial vehicle," *Applied Mechanics and Materials*, Vol. 629, 2014, pp. 152-157.
- [11] Elahinia MH, Shape Memory Alloy Actuators: Design, Fabrication and Experimental Evaluation. Hoboken, New Jersey, John Wiley & Sons, 2016.
- [12] Martinez-Lucci J, Amano RS, Rohatgi P, "Review in self-healing in metal matrix composites," *Journal of Aeronautics, Astronautics and Aviation*, Vol. 53, No. 4, 2021, pp. 441-472.
- [13] Scherngell H, Kneissl AC, "Generation, development and degradation of the intrinsic two-way shape memory effect in different alloy systems," *Acta Materialia*, Vol. 50, No. 2, 2002, pp. 327-341.
- [14] Lambert TR, Modeling and Numerical Simulation of Shape Memory Alloys in Robotics Applications. PhD Thesis, Auburn University, 2017.
- [15] Kauffman GB, Mayo I, "The story of nitinol: the serendipitous discovery of the memory metal and its applications," *The Chemical Educator*, Vol. 2, 1997, pp. 1-21.
- [16] Karakalas AA, Machairas TT, Lagoudas DC, Saravanos DA, "Design of morphing strips using sma actuators under partial phase transformation operation," *Smart Materials, Adaptive Structures and Intelligent Systems*, Vol. 84027, 2020.
- [17] Qidwai MA, Lagoudas DC, "Numerical implementation of a shape memory alloy thermomechanical constitutive model using return mapping algorithms," *International Journal for Numerical Methods in Engineering*, Vol. 47, No. 6, 2000, pp. 1123-1168.
- [18] Hartl DJ, Lagoudas DC, "Characterization and 3-D modeling of Ni60Ti SMA for actuation of a variable geometry jet engine chevron," *Sensors and Smart Structures Technologies for Civil, Mechanical, and Aerospace Systems*, Vol. 6529, 2007, pp. 1212-1223.
- [19] Contreras MM, Design, Analysis and Control of A Nitinol Shape Memory Alloy Rotary Actuator for Spacecraft Deployable Structures. PhD Thesis, Massachusetts Institute of Technology, 2019.
- [20] Huang W, "On the selection of shape memory alloys for actuators," *Materials & Design*, Vol. 23, No. 1, 2002, pp. 11-19.
- [21] Kumar D, Daudpoto J, Chowdhry BS, "Challenges for practical applications of shape memory alloy actuators," *Materials Research Express*, Vol. 7, No. 7, 2020, 073001.
- [22] Lara-Quintanilla A, Bersee HEN, "Active cooling and strain-ratios to increase the actuation frequency of SMA wires," *Shape Memory and Superelasticity*, Vol. 1, 2015, pp. 460-467.
- [23] Tadesse Y, Thayer N, Priya S, "Tailoring the response time of shape memory alloy wires through active cooling and pre-stress," *Journal of Intelligent Material Systems and Structures*, Vol. 21, No. 1, 2010, pp. 19-40.
- [24] Otieno T, Shape Memory Alloy Actuator for Cross-Feed in Turning Operation. Master's Thesis, Nelson Mandela Metropolitan University, 2012.
- [25] Langbein S, Czechowicz A, "Problems and solutions for shape memory actuators in automotive applications," *Smart Materials, Adaptive Structures and Intelligent Systems*, Vol. 45103, 2012, pp. 433-439.
- [26] Koh JS, "Design of shape memory alloy coil spring actuator for improving performance in cyclic actuation," *Materials*, Vol. 11, No. 11, 2018, 2324.
- [27] Kim SH, Lima MD, Kozlov ME, Haines CS, Spinks GM, Aziz S, Choi C, Sim HJ, Wang X, Lu H, Qian D, "Harvesting temperature fluctuations as electrical energy using torsional and tensile polymer muscles," *Energy & Environmental Science*, Vol. 8, No. 11, 2015, pp. 3336-3344.
- [28] Avirovik D, Kishore RA, Vuckovic D, Priya S, "Miniature shape memory alloy heat engine for powering wireless sensor nodes," *Energy Harvesting and Systems*, Vol. 1, No. 1-2, 2014, pp. 13-18.
- [29] Duerig TW, Engineering Aspects of Shape Memory Alloys. Oxford, Butterworth-Heinemann, 1990.